



Published in final edited form as:

J Surg Res. 2014 August ; 190(2): 628–633. doi:10.1016/j.jss.2014.05.011.

Far-Red Tracer Analysis of Traumatic Cerebrovascular Permeability

George P Liao, MD, Scott D Olson, PhD, Daniel J Kota, PhD, Robert A Hetz, MD, Philippa Smith, BA, BS, Supinder Bedi, PhD, and Charles S Cox Jr, MD

Department of Pediatric Surgery, University of Texas Health Science Center at Houston 6431 Fannin Street, MSB 5.230, Houston, TX 77030, USA

Abstract

Introduction—Blood brain barrier (BBB) compromise is a key pathophysiological component of secondary traumatic brain injury characterized by edema and neuroinflammation in a previously immune privileged environment. Current assays for BBB permeability are limited by working size, harsh extraction processes, suboptimal detection via absorbance, and wide excitation fluorescence spectra. In this study, we evaluate the feasibility of Alexa Fluor 680, a far-red dye bioconjugated to dextran, as an alternative assay to improve resolution and sensitivity.

Methods—Alexa Fluor was introduced intravenously on day of sacrifice to three groups: Sham, Controlled Cortical Injury (CCI), and CCI treated with a cell based therapy known to reduce BBB permeability. The brains were sectioned coronally and imaged using an infrared laser scanner to generate intensity plot profiles as well as signal threshold images to distinguish regions with varying degrees of permeability.

Results—Linear plot profile analysis demonstrated greater signal intensity from CCI than treated rats at corresponding injury depths. Threshold analysis identified rims of signal at low + narrow threshold ranges. The integrated signals from a treatment group known to preserve the BBB were significantly less than the groups with CCI injury alone. There was no significant difference at high + wide signal intensity threshold ranges.

© 2014 Elsevier Inc. All rights reserved.

Correspondence and address for reprints (reprints will be ordered): George Paul Liao, MD, 6431 Fannin, MSB 5.230, Houston, TX 77030, George.P.Liao@uth.tmc.edu.

Off-label Use: none

Conflict of Interest: none

Author's contribution: Conception and design: SDO, CSC, RAH, GPL, PS, DJK

Analysis and interpretation: GPL, PS

Data collection: GPL, RAH, PS

Writing the article: GPL, SDO, CSC

Critical revision of the article: SDO, CSC

Obtaining funding: CSC

Publisher's Disclaimer: This is a PDF file of an unedited manuscript that has been accepted for publication. As a service to our customers we are providing this early version of the manuscript. The manuscript will undergo copyediting, typesetting, and review of the resulting proof before it is published in its final citable form. Please note that during the production process errors may be discovered which could affect the content, and all legal disclaimers that apply to the journal pertain.

Conclusions—Alexa Fluor 680 infrared photodetection and image analysis can aid in detecting differential degrees of BBB permeability following traumatic brain injury and may be particularly useful in demonstrating BBB preservation of at-risk regions in response to therapeutic agents.

Keywords

Traumatic Brain Injury; Blood Brain Barrier; Fluorescence; Edema; Permeability

INTRODUCTION

Severe traumatic brain injury (TBI) defined as a Glasgow Coma Scale of 3–8 continues to carry high morbidity in the pediatric and adult population with limited diagnostic and treatment modalities. Blood Brain barrier (BBB) permeability and cerebral edema play crucial roles in the pathophysiological progression of secondary injuries following TBI, and are clinically manifest as increased intracranial pressure and reduced cerebral perfusion pressure. BBB compromise leads to vasogenic edema, exposing the previously immunoinflammatory privileged cerebral tissue to an influx of inflammatory factors and cells¹. Cytotoxic edema co-exists and is the result of the cellular insult and the loss of the ability to maintain intracellular volume².

The injury penumbra has been previously described by our laboratory and collaborators as tissue adjacent to the area of injury, and characterized by the presence of neuroinflammatory cells and proinflammatory cytokines³. The condition of the BBB in this at-risk region of brain is likely in transition between healthy and dysfunctional cerebral microvasculature and can be evaluated in the preclinical setting via excess tissue water (cerebral edema) and dye extravasation (increased microvascular permeability). Clinically, BBB compromise can be estimated via microdialysis catheters or external ventricular drains as ratios between brain and serum total protein or albumin levels⁴. However, direct preclinical and clinical visualization of penumbral BBB permeability in situ has been limited to imaging modalities such as diffusion tensor magnetic resonance imaging. . Active research exists in identifying and targeting therapy to rescue these at-risk regions.

In preclinical studies, the simplest method of indirectly assessing the degree of blood brain barrier dysfunction is brain water content, which offers global differences and is subject to variations in animal sacrifice technique and post mortem handling of brain tissue⁵. Evans Blue dye extravasation, a popular assay used to study the BBB response following TBI has affinity to the 66kDa albumin. Thus under normal circumstances, Evans Blue dye remains in circulation because of the 0.4kDa pore size of the BBB. Following TBI, BBB compromise causes Evans Blue extravasation into the interstitial tissue and can be quantified after extraction^{6–8}. We, along with our collaborators have previously used tissue water, Evans Blue as well as immunohistochemistry to demonstrate that cell based therapies can modulate the neuroinflammatory response following TBI resulting in penumbral BBB preservation^{9–11}. Of note, Pati et al demonstrated in mouse models of TBI that mesenchymal stem cells exert perivascular protective effects to the penumbral BBB via increased junctional protein (VE-cadherin and occluding) expression¹². Walker et al showed increased localization/organization of occludins to the microvasculature¹³.

Despite wide use in TBI research, the utility of Evans Blue is limited due to several factors. The first is the relatively large molecular size of albumin compared to the BBB pore size. Second, the detection of extracted Evans Blue uses absorbance, a suboptimal detection process complicated by a wide excitation fluorescence spectrum. Third, the harsh extraction process destroys brain tissue and precludes further histologic analysis on the same tissue sample.

Alexa Fluor (Lifetechnologies, Carlsbad, CA) is a fluorescent marker that has been conjugated to a variety of molecules and has been used in investigations for drug transit across the BBB¹⁴. Highly sensitive, high resolution infrared laser scanners can detect subtle changes in signal intensities of Alexa Fluor between adjacent anatomical structures in brain tissue samples. We have previously demonstrated that Alexa Fluor reduces the non-specific signal between sham and injury to 7% ($p < 0.001$), an eightfold reduction (Figure 1). The high sham signal for Evans Blue is likely due to the tissue handling and the extraction process where extraparenchymal and intravascular Evans Blue dye cannot be easily excluded from intraparenchymal dye when placed under an absorbance microplate reader. The goal of our study was to evaluate Alexa Fluor 680, a far-red dye bioconjugated to dextran (10kDa) as an alternative, to Evans Blue in order to expand research capabilities with a multimodal detection assay that increases the sensitivity to BBB perturbations, allowing the identification and quantification of at-risk penumbral areas of microvascular injury, and preserving tissue for further assays.

MATERIALS AND METHODS

All protocols involving the use of animals were in compliance with the National Institutes of Health *Guide for the Care and Use of Laboratory Animals* and were approved by the University of Texas Institutional Animal Care and Use Committee (protocol HSC-AWC-11-120).

Surgical study design

The three groups in this study were Sham (n=10), Controlled Cortical Impact (CCI) (n=10) and Treatment (n=10). All groups received Alexa Fluor intravenously at time of euthanasia. Each group underwent our acute traumatic brain injury model, undergoing their respective injury at time zero followed by euthanasia at 72 hours. In this study, the treatment group received human adult bone-marrow derived stromal cells that we previously showed by Evans Blue and tissue water assays to reduce post TBI BBB permeability^{9,10}. The treatment group received the cell based product at 24 and 48 hours post injury via tail vein injection.

Controlled Cortical Impact and Sham Injuries

A CCI device (Leica Impact One Stereotaxic Impactor, Buffalo Grove, IL) was used to administer unilateral brain injuries as described previously by Lighthall.¹⁵ Briefly, male rats weighing 225–250g were anesthetized with 4% isoflurane and oxygen. The rats were shaved and prepped, then mounted and secured on a stereotaxic frame in the horizontal plane. After subcutaneous infiltration of 0.25% bupivacaine, a midline incision was made and extended in depth to the skull. A 7–8mm craniectomy centered between the bregma and lambda

sutures was performed to the right cranial vault approximately 3mm lateral to the midline to expose the tempoparietal cortex. The impact parameters included a 6mm diameter tip positioned orthogonal to the cortex at an angle of 10 degrees off the vertical plane with a deformation depth of 3.1mm at a velocity of 5.8m/s and a dwell time of 200ms. This impact created a severe traumatic brain injury to the parietal association cortex. Sham injuries were performed in an identical fashion, but excluded craniectomy and injury. All incisions were closed using sterile surgical clips.

Alexa Fluor 680 dye BBB permeability analysis

At euthanasia, rats were anesthetized as described above and 1mg/kg of Alexa Fluor 680 dye conjugated to 10kDa dextran in PBS was introduced via tail vein injection. The animals were allowed to recover for 30 minutes, then sacrificed via right cardiac puncture and perfused with ice cold PBS followed by 4% PFA. Explanted brains were placed in 4% PFA for one hour, and then transferred to PBS. The brains were then sectioned coronally into 1mm slices using a rat brain matrix slicer (Zivic Instruments, Pittsburgh, PA). Eight anatomically standardized slices encompassing the area of injury are placed on a plastic petri dish using a grid and imaged using a LI-COR Odyssey CLx infrared laser scanner (LI-COR, Lincoln, Nebraska) at 700 and 800nm. Raw images were then stacked, processed and analyzed in batch using Fiji¹⁶, the fully open source version of ImageJ 1.48p(<http://imagej.nih.gov/ij>). A 700nm (Alexa 680) and 800nm (background) channel merged montage of a representative brain from each treatment group is shown in Figure 2.

Plot profiles were generated for each slice along the impactor trajectory to identify the depth and anatomical region corresponding to the maximum Alexa Fluor signal intensity. The one dimensional plot of Alexa Fluor signal intensity suggested that there may be two to three dimensional regions of BBB permeability following TBI corresponding to the injury penumbra (Figure 3). To identify potential regions of BBB permeability, threshold ranges were applied to the stacked raw images to detect various regional patterns of Alexa Fluor signal arising from the brain tissue from the site of cortical impact. Low + narrow signal intensity threshold ranges identified rims surrounding the area of maximal injury (4000–5000, 5000–7500, 5000–10,000) while high + wide signal intensity threshold ranges identified the highest foci of signal within the most injured area of the cortex (10,000 to 60,000). For each rat brain, the area of integrated signal from the Alexa Fluor was plotted against these intensity threshold ranges.

Data Analysis

Group data were expressed as means \pm 95% confidence interval. Plot profile analysis for maximum intensity was analyzed with one way ANOVA with Tukey's multiple comparison test. Comparisons of BBB permeability between CCI and treated groups using intensity thresholds was analyzed with two-tailed t tests

RESULTS

Plot Profile Analysis

The linear plot profile technique identified the maximum intensity and its depth from the surface. The mean maximum signal for CCI rats 6579 ± 2371 was significantly greater than Sham 1478 ± 218 ($p < 0.0001$) as well as the treated rats 3701 ± 1699 vs. ($p = 0.04$). For the CCI animals, the distance to the maximum signal was 2.0 ± 0.6 mm while in the treated rats the distance was 1.7 ± 0.4 mm, which was not significantly different ($p = 0.282$).

At-risk BBB Permeability Region Identification and Quantification

The integrated signal generated for regions using ranges of intensity thresholds identified rim patterns corresponding to the penumbra as well as focal patterns corresponding to areas of maximal injury within the cortex (Figure 4). One CCI rat brain was not analyzed as the tissue was lost during processing. The analysis identified two treatment animals that had 10 fold intensity levels throughout the brain, likely due to inadequate perfusion or flushing of the circulation at sacrifice, thus were excluded from the analysis. Significant differences in integrated signal between CCI ($n = 9$) and treated animals ($n = 8$) was identified in the low + narrow threshold range of 4000–5000 (1451 ± 267 vs. 1041 ± 224 , $p = 0.016$), 5000–7500 (2389 ± 605 vs. 1496 ± 409 , $p = 0.015$), and 5000–10,000 (3214 ± 878 vs. 2043 ± 679 , $p = 0.030$). These ranges were presumed to be penumbral regions based on their morphology of concentric rims surrounding the core of maximal injury as well as the low + narrow intensity signals suggesting that the identified area retained some BBB function. There was no significant difference in the integrated signal between CCI ($n = 9$) and treated ($n = 8$) animals in the high + wide signal intensity threshold range of 10,000 to 60,000 (797 ± 971 vs. 345 ± 377 , $p = 0.354$) presumed to be core foci of contusion, hemorrhage and/or complete BBB disruption (Figure 5).

DISCUSSION

This study demonstrated that the Alexa Fluor 680 dye conjugated to 10kDa dextran can be used in preclinical studies of traumatic brain injury to suggest the location and degree of BBB permeability associated with at-risk penumbral regions. Applying the low + narrow intensity threshold range identifies a rim of penumbral tissue that may be the subtle transition zone of BBB permeability and allows quantitative as well as morphologic tracking of the treatment response. Co-localization studies on the same tissue samples may then be used to evaluate the integrity of the cells and junctional proteins comprising the BBB.

The pathophysiology of traumatic brain injury is complex, and edema is just one component¹⁷. Previously, tissue water and Evans Blue analysis could only offer global insight into the aggregate injury to the micro- (cerebral vasculature) and sub-microvasculature (BBB)¹⁸. For the study of vasogenic edema and associated neuroinflammation, Evans Blue may be limited to the size of albumin. Albumin alone may not detect the subtle changes to signal intensity to at-risk regions along the trajectory of impact seen in this study. Alexa Fluor 680 is also available commercially, conjugated to 6kDa dextran, which may provide even greater sensitivity to BBB perturbations.

Whole brain slice imaging and image analysis has many advantages over tissue water and Evans Blue analysis. Infrared image scanning precludes the need of detaching contralateral hemispheres for normalization and decreases signal to noise. Although the Alexa Fluor dye is considerably more expensive than Evans Blue, maintaining intact brain architecture allows for immunohistochemistry. Furthermore, the infrared fluorescence range of Alexa Fluor allows for the use of more fluorescent markers per sample and for the tissue to be potentially used for flow cytometry.

There are limitations to tissue processing using Alexa Fluor. The slicing matrix currently limits the slicing technique to a thickness of 1mm. At this thickness, slicing the brain tissue necessitates sequential placing of razor blades from posterior to anterior at 1mm depth into brain tissue and then advancing all blades completely into the matrix grooves simultaneously. Standardizing which 8 slices are to be imaged is reproducible and in our lab involves laying out all the blades with their individual slices and identifying the three slices that contain the mammillary nucleus and median eminence. After these slices are identified, the three preceding posterior slices and two proceeding anterior slices are included to form the 8 standardized slices. The success of the resulting slices does depend on the condition of the explanted brain. Any pre-existing cuts or defects can produce suboptimal slices. The image analysis software can then calculate the area of each slice and the 1mm slices can be summed to estimate brain volume.

In our study, plot profiles were generated along a line connecting the cortical surface (orthogonal to the impactor) to the center of the third ventricle. The maximum intensity was identified and its depth from the cortex noted. While there was no difference between the depth between CCI and treatment groups, the intensity levels were found to be significantly different. This finding suggests that the cell based treatment may be attenuating the BBB permeability or reducing the neuroinflammatory response at a depth that corresponds to the interface between the cortex and the hippocampus.

The image analysis process for Alexa Fluor allows for previously unobtainable capabilities but also has limitations. A scatter plot showing integrated density versus area across series of single rat brains can validate the uniformity of the injury and of slicing. The threshold selection process can be a significant limitation due to subjectivity, but can be standardized using predetermined anatomic parameters such as penumbra selection or criteria that can be applied across experiments such as same threshold ranges. In this study, the low + narrow threshold range identified potential penumbral areas and showed significant treatment effects in these areas compared to CCI rats. These findings suggest less penumbral BBB permeability in treated rats versus rats with CCI injury alone. Despite variability in injury size created by surgery, as evidence by the spread of the data points in Figure 5, the consistent trend of the penumbral signals still allows for significance to be reached amongst a heterogeneous collection of injuries. The small foci identified at the 10,000–60,000 intensity range likely represents tissue with significant dysfunction in permeability regulation or devitalized tissue as seen with intraparenchymal contusions or microvascular hemorrhage. The principles of identifying areas of BBB compromise and edema can be translated into clinical practice. In 2006, Lescot et al used computed tomography to measure volume, weight and specific gravity of contused and noncontused areas in patients with

severe traumatic brain injury¹⁹. Recently, preclinical investigators using MRI with diffusion weighted imaging (DWI) technology have been able to identify temporal and regional differences in edema following traumatic brain injury in rabbits. The authors were able to differentiate between vasogenic and cytotoxic edema based on higher or lower apparent diffusion coefficients respectively²⁰. Newcombe et al applied diffusion tensor MRI to at-risk contusions in acute post TBI patients and found a pattern of concentric regions of varying diffusion similar to our Alexa Fluor findings. The authors suggested that the outermost rim of hypodensity “may represent a ‘traumatic penumbra’ which may be rescued by effective therapy”²¹. The ability to identify differential degrees of BBB permeability using Alexa Fluor can serve as an additional useful preclinical assay for investigators in the development and evaluation of potential stereotactic or systemically delivered therapeutics.

In conclusion, our study demonstrates that the Alexa Fluor 680 conjugated to dextran assay is sensitive, specific and provides a platform for brain slice imaging and analysis. This technique identifies regional changes in BBB permeability and may be used to track the response of at-risk regions to potential therapeutics. Our future studies will employ MRI and immunohistochemistry used in tandem with Alexa Fluor 680 to not only evaluate BBB permeability across different imaging modalities but also provide internal validation. Rat brains will be first imaged in vivo with MRI prior to sacrifice to map out the penumbral area of BBB permeability. The brains will then be perfused with Alexa Fluor 680, explanted, sectioned, imaged and then analyzed using the low + narrow intensity signal threshold range parameters described in this study. The same sections can then be stained with immunohistochemistry to identify markers known to be involved in BBB permeability. Images acquired from these three modalities can be overlaid to confirm that the same at risk region has been identified. Lastly, we anticipate that Alexa Fluor can be potentially applied beyond TBI in research, detecting increased microvascular permeability of at risk regions in cardiac tissue following myocardial infarction or in brain tissue following stroke.

References

1. Barzo P, Marmarou A, Fatouros P, Hayasaki K, Corwin F. Contribution of vasogenic and cellular edema to traumatic brain swelling measured by diffusion-weighted imaging. *Journal of neurosurgery*. Dec; 1997 87(6):900–907. [PubMed: 9384402]
2. Pasco A, Lemaire L, Franconi F, et al. Perfusional deficit and the dynamics of cerebral edemas in experimental traumatic brain injury using perfusion and diffusion-weighted magnetic resonance imaging. *Journal of neurotrauma*. Aug; 2007 24(8):1321–1330. [PubMed: 17711393]
3. Harting MT, Jimenez F, Adams SD, Mercer DW, Cox CS Jr. Acute, regional inflammatory response after traumatic brain injury: Implications for cellular therapy. *Surgery*. Nov; 2008 144(5):803–813. [PubMed: 19081024]
4. Saw MM, Chamberlain J, Barr M, Morgan MP, Burnett JR, Ho KM. Differential Disruption of Blood-Brain Barrier in Severe Traumatic Brain Injury. *Neurocritical care*. Nov 14, 2013
5. van den Brink WA, Marmarou A, Avezaat CJ. Brain oedema in experimental closed head injury in the rat. *Acta neurochirurgica Supplementum*. 1990; 51:261–262. [PubMed: 2089912]
6. Imer M, Omay B, Uzunkol A, et al. Effect of magnesium, MK-801 and combination of magnesium and MK-801 on blood-brain barrier permeability and brain edema after experimental traumatic diffuse brain injury. *Neurological research*. Nov; 2009 31(9):977–981. [PubMed: 19215660]
7. Terpolilli NA, Kim SW, Thal SC, Kuebler WM, Plesnila N. Inhaled nitric oxide reduces secondary brain damage after traumatic brain injury in mice. *Journal of cerebral blood flow and metabolism* :

- official journal of the International Society of Cerebral Blood Flow and Metabolism. Feb; 2013 33(2):311–318.
8. Khan M, Im YB, Shunmugavel A, et al. Administration of S-nitrosoglutathione after traumatic brain injury protects the neurovascular unit and reduces secondary injury in a rat model of controlled cortical impact. *Journal of neuroinflammation*. 2009; 6:32. [PubMed: 19889224]
 9. Walker PA, Shah SK, Jimenez F, Aroom KR, Harting MT, Cox CS Jr. Bone marrow-derived stromal cell therapy for traumatic brain injury is neuroprotective via stimulation of non-neurologic organ systems. *Surgery*. Nov; 2012 152(5):790–793. [PubMed: 22853856]
 10. Walker PA, Bedi SS, Shah SK, et al. Intravenous multipotent adult progenitor cell therapy after traumatic brain injury: modulation of the resident microglia population. *Journal of neuroinflammation*. 2012; 9:228. [PubMed: 23020860]
 11. Pati S, Khakoo AY, Zhao J, et al. Human mesenchymal stem cells inhibit vascular permeability by modulating vascular endothelial cadherin/beta-catenin signaling. *Stem cells and development*. Jan; 2011 20(1):89–101. [PubMed: 20446815]
 12. Menge T, Zhao Y, Zhao J, et al. Mesenchymal stem cells regulate blood-brain barrier integrity through TIMP3 release after traumatic brain injury. *Science translational medicine*. Nov 21. 2012 4(161):161ra150.
 13. Walker PA, Shah SK, Jimenez F, et al. Intravenous multipotent adult progenitor cell therapy for traumatic brain injury: preserving the blood brain barrier via an interaction with splenocytes. *Experimental neurology*. Oct; 2010 225(2):341–352. [PubMed: 20637752]
 14. Nuriya M, Shinotsuka T, Yasui M. Diffusion properties of molecules at the blood-brain interface: potential contributions of astrocyte endfeet to diffusion barrier functions. *Cereb Cortex*. Sep; 2013 23(9):2118–2126. [PubMed: 22776675]
 15. Lighthall JW. Controlled cortical impact: a new experimental brain injury model. *Journal of neurotrauma*. 1988; 5(1):1–15. [PubMed: 3193461]
 16. Schindelin J, Arganda-Carreras I, Frise E, et al. Fiji: an open-source platform for biological-image analysis. *Nature methods*. Jul; 2012 9(7):676–682. [PubMed: 22743772]
 17. Neuwelt EA, Bauer B, Fahlke C, et al. Engaging neuroscience to advance translational research in brain barrier biology. *Nature reviews. Neuroscience*. Mar; 2011 12(3):169–182.
 18. Taya K, Marmarou CR, Okuno K, Prieto R, Marmarou A. Effect of secondary insults upon aquaporin-4 water channels following experimental cortical contusion in rats. *Journal of neurotrauma*. Jan; 2010 27(1):229–239. [PubMed: 19705963]
 19. Lescot T, Degos V, Zouaoui A, Preteux F, Coriat P, Puybasset L. Opposed effects of hypertonic saline on contusions and noncontused brain tissue in patients with severe traumatic brain injury. *Critical care medicine*. Dec; 2006 34(12):3029–3033. [PubMed: 16971850]
 20. Wei XE, Zhang YZ, Li YH, Li MH, Li WB. Dynamics of rabbit brain edema in focal lesion and perilesion area after traumatic brain injury: a MRI study. *Journal of neurotrauma*. Sep 20; 2012 29(14):2413–2420. [PubMed: 21675826]
 21. Newcombe VF, Williams GB, Outtrim JG, et al. Microstructural basis of contusion expansion in traumatic brain injury: insights from diffusion tensor imaging. *Journal of cerebral blood flow and metabolism : official journal of the International Society of Cerebral Blood Flow and Metabolism*. Jun; 2013 33(6):855–862.

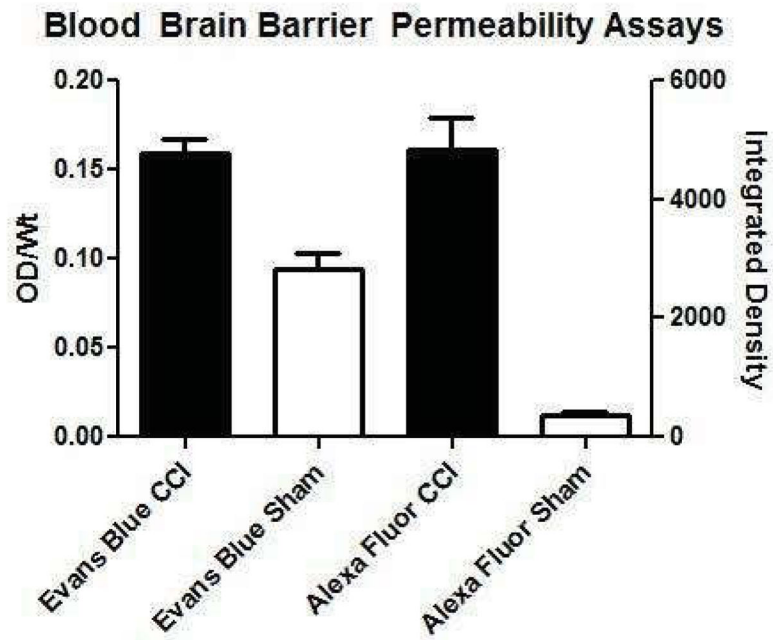


Figure 1.

Non-specific signals are reduced with Alexa Fluor compared to Evans Blue dye as evidenced by the high signal from sham animals receiving Evans Blue. Evans Blue CCI (n=11), Evans Blue Sham (n=6), Alexa Fluor CCI (n=9), Alexa Fluor Sham (n=10). The Y axis OD/Wt refers to optical density (absorbance) per rat weight. The X axis Integrated Density refers to the cumulated signal detected by the far-red scanner across the brain slices.

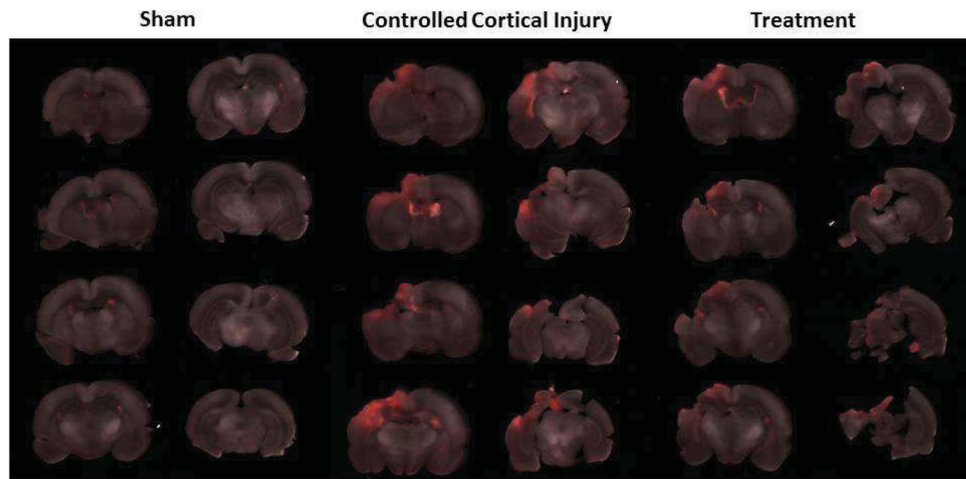


Figure 2.

A representative montage containing the three experimental groups after merging the two detection channels (700nm - Alexa 680 and 800nm - background). Red areas represent presence of Alexa-Fluor 680 dye.

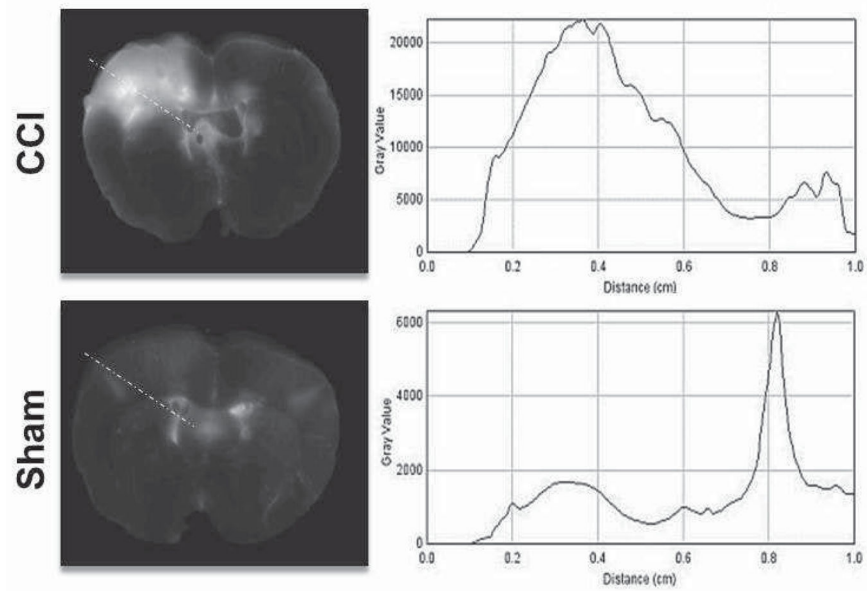


Figure 3. One dimensional signal intensity along the impact trajectory represented as an orthogonal line connecting the cortical surface to the 3rd ventricle. The signal intensity can serve as a surrogate for blood brain barrier permeability along the depth of injury.

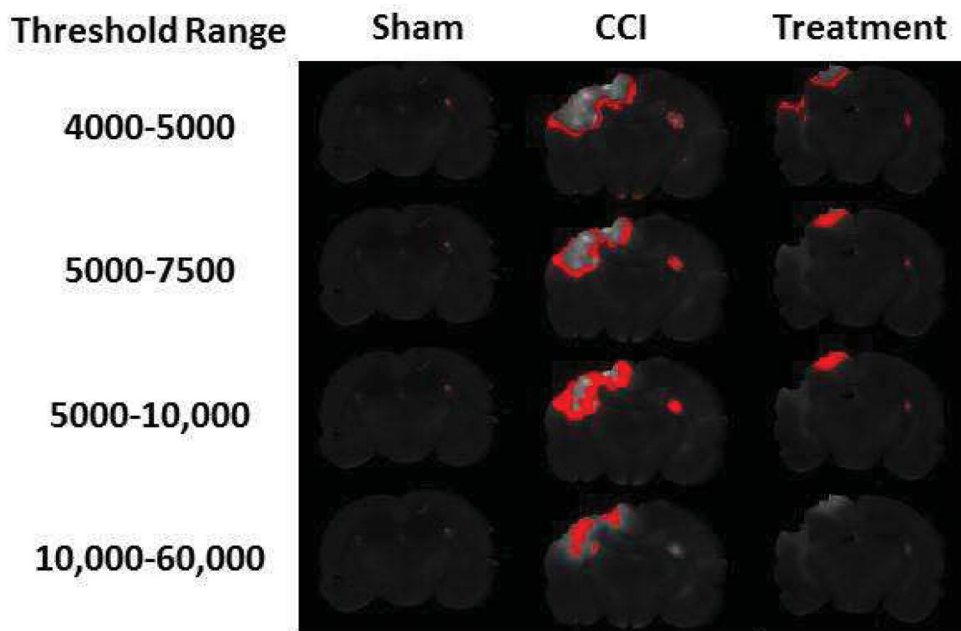


Figure 4.

The same representative slice from each of the three experimental groups used in Figure 1 with the application of 4 different intensity thresholds to represent the three low + narrow threshold ranges corresponding to penumbral areas and the one high + wide threshold range representing foci of hemorrhage/contusion/complete BBB disruption. The integrated signals from the treated rats were significantly less than CCI rats, suggesting a therapeutic effect on the penumbral regions.

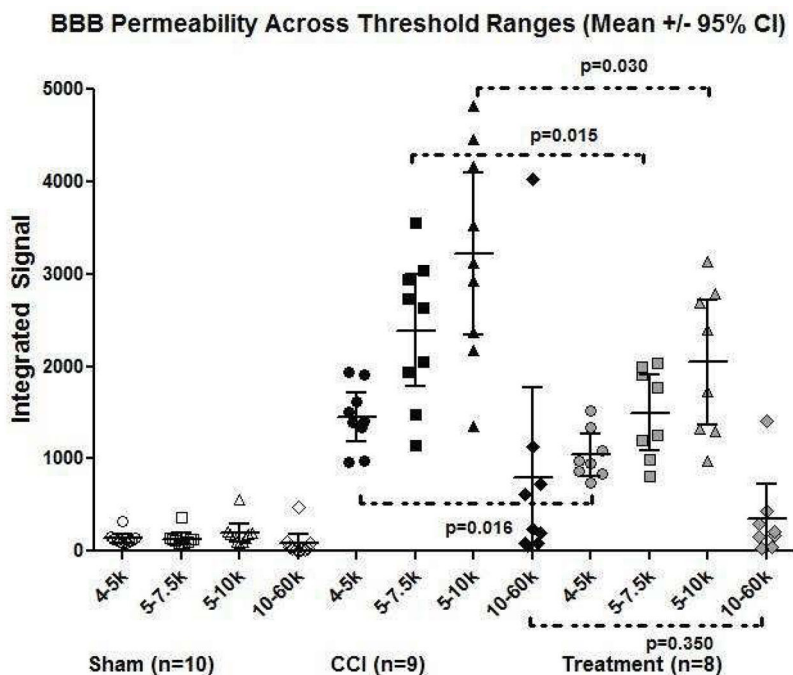


Figure 5.

A scatter plot representation of Figure 4 demonstrates integrated signal across each threshold intensity range for the three experimental groups. Despite the wide spread within each treatment group suggesting heterogeneity of injury, there is a consistent trend within each treatment group from the three low + narrow threshold ranges to the one high + wide threshold range. A significant therapeutic effect is seen between treated versus CCI rats in the low + narrow threshold ranges, which correspond to the red rims identified in Figure 4 (likely at-risk penumbral regions of BBB permeability).